RESEARCH PAPER

Cancer Biology & Therapy 11:2, 263-276; January 15, 2011; © 2011 Landes Bioscience

Anticancer activity of celastrol in combination with ErbB2-targeted therapeutics for treatment of ErbB2-overexpressing breast cancers

Srikumar M. Raja,[1,4,*] Robert J. Clubb,[1,4,†] Cesar Ortega-Cava,[1,4] Stetson H. Williams,[1] Tameka A. Bailey,[1] Lei Duan,[1,4,‡] Xiangshan Zhao,[3,4] Alagarasamy L. Reddi,[4,¥] Abijah M. Nyong,[1] Amarnath Natarajan,[1] Vimla Band[1,3,4] and Hamid Band[1-4,*]

[1]Eppley Institute for Research in Cancer and Allied Diseases; [2]Departments of Biochemistry and Molecular Biology, Pathology and Microbiology, and Pharmacology and Neuroscience; and [3]Genetics, Cell Biology and Anatomy; College of Medicine; University of Nebraska Medical Center; Omaha, NE USA

This work was initiated while the indicated authors were in the: [4]Department of Medicine, Evanston Northwestern Healthcare Research Institute, Northwestern University, Evanston, IL USA

Current address: [†]Genzyme Genetics; Westborough, MA USA; [‡]Rush University Medical Center; Chicago, IL USA; [¥]Department of Medicine; Northwestern University; Chicago, IL USA

Key words: ErbB2, Her2/Neu, 17-AAG, celastrol, trastuzumab, targeted therapy, drug interaction, ubiquitin, proteasome, HSP90, ROS

Abbreviations: AR, androgen receptor; 17-AAG, 17-(allylamino)-17-demethoxygeldanamycin; CI, combination index; CIM, confocal immunofluorescence microscopy; CM-H_2DCFDA, 5-(and-6)-chloromethyl-2'-7'-dichlorodihydrofluorescein diacetate, acetyl ester; DAPI, 4', 6-diamidino-2-phenylindole; DTT, dithiothreitol; ErbB2 or Her2, epidermal growth factor receptor B2 or human epidermal growth factor receptor 2; Her3, human epidermal growth factor receptor 3; EGF, epidermal growth factor; EGFR, epidermal growth factor receptor; ER, endoplasmic reticulum; FACS, fluorescence activated cell sorter; GA, geldanamycin; GSH, reduced glutathione; HSP90, heat shock protein 90; Hsc70, heat shock cognate 70; IKK, Ikappa B kinase; IP, immunoprecipitation; IF, immunofluorescence; IB, immunoblotting; MEM, minimal essential media; MTT, 3-(4,5-dimethylthiazol-2-yl)-2,5-diphenyltetrazoliumbromide; NFκB, nuclear factor kappaB; LAMP-1, lysosome associated membrane protein-1; PEITC, phenyl ethyl isothiocyanate; PFA, paraformaldehyde; PI3K, phospho-inositide-3-kinase; PTEN, phosphatase and tensin homolog deleted on chromosome ten; ROS, reactive oxygen species; RTK, receptor tyrosine kinase; SDS-PAGE/WB, sodium dodecylsulfate polyacrylamide gel electrophoresis/western blotting; Ub, ubiquitin; UPR, unfolded protein response

The receptor tyrosine kinase ErbB2 is overexpressed in up to a third of breast cancers, allowing targeted therapy with ErbB2-directed humanized antibodies such as Trastuzumab. Concurrent targeting of ErbB2 stability with HSP90 inhibitors is synergistic with Trastuzumab, suggesting that pharmacological agents that can inhibit HSP90 as well as signaling pathways activated by ErbB2 could be useful against ErbB2-overexpressing breast cancers. The triterpene natural product Celastrol inhibits HSP90 and several pathways relevant to ErbB2-dependent oncogenesis including the NFκB pathway and the proteasome, and has shown promising activity in other cancer models. Here, we demonstrate that Celastrol exhibits in vitro antitumor activity against a panel of human breast cancer cell lines with selectivity towards those overexpressing ErbB2. Celastrol strongly synergized with ErbB2-targeted therapeutics Trastuzumab and Lapatinib, producing higher cytotoxicity with substantially lower doses of Celastrol. Celastrol significantly retarded the rate of growth of ErbB2-overexpressing human breast cancer cells in a mouse xenograft model with only minor systemic toxicity. Mechanistically, Celastrol not only induced the expected ubiquitinylation and degradation of ErbB2 and other HSP90 client proteins, but it also increased the levels of reactive oxygen species (ROS). Our studies show that the Michael Acceptor functionality in Celastrol is important for its ability to destabilize ErbB2 and exert its bioactivity against ErbB2-overexpressing breast cancer cells. These studies suggest the potential use of Michael acceptor-containing molecules as novel therapeutic modalities against ErbB2-driven breast cancer by targeting multiple biological attributes of the driver oncogene.

*Correspondence to: Srikumar M. Raja and Hamid Band; Email: sraja@unmc.edu and hband@unmc.edu
Submitted: 07/28/10; Revised: 09/27/10; Accepted: 10/16/10
DOI: 10.4161/cbt.11.2.13959

Introduction

ErbB2 (Her2/Neu), one of the four Epidermal Growth Factor Receptor family members, is overexpressed in a number of human malignancies; ErbB2-overexpression is found in nearly a third of all breast cancers.[1,2] ErbB2-overexpressing breast cancers represent a distinct molecular subtype with an especially poor outcome,[3,4] necessitating newer forms of therapy. Expression of ErbB2 on the cell surface, together with its essential role in driving oncogenesis, has led to its successful targeting with humanized anti-ErbB2 antibodies such as Trastuzumab (Herceptin™).[1,2,5,6] However, de novo as well as acquired resistance to Trastuzumab is a serious issue.[5-8] Some identified resistance factors, including PI3-kinase pathway activation due to PTEN inactivation and upregulation of RTKs such as Insulin-like growth factor receptor I, EGFR or ErbB3 have suggested combinations of targeted therapies.[2,7,9,10] However, agents that can target biological attributes of ErbB2 or can target essential oncogenic signaling pathways downstream of ErbB2 represent alternate approaches to enhance the effects of ErbB2 targeted therapeutics to eventually reduce or overcome resistance.

Heat shock protein 90 (HSP90) is essential for stability of ErbB2 as well of a number of signaling proteins such as p-Akt, c-Raf-1, c-Src and Hif-1α that are components of ErbB2-driven signaling.[11,12] Indeed, we have recently shown that a combination of Trastuzumab and an HSP90 inhibitor 17-allylaminodemethoxy geldanamycin (17-AAG) synergistically and selectively induces growth arrest and cytotoxicity in ErbB2-overexpressing breast cancer cells.[13] These findings are of potential clinical significance since 17-AAG and other HSP90 inhibitors are now undergoing phase II clinical evaluation in various cancers, including ErbB2-driven breast cancer.[14-16] While selective HSP90 inhibitors hold significant promise, recent reports also indicate the ability of 17-AAG to transiently activate c-Src signaling and promote bone metastasis.[17] Therefore new agents that modulate HSP90 function but possess additional anticancer effects could substantially aid in designing combinatorial therapeutics against ErbB2-overexpressing cancers.

Recent studies in prostate cancer cells showed that the Chinese herbal product Celastrol induces a gene expression signature that overlaps with the HSP90 inhibitor-induced gene expression signature; furthermore, Celastrol induced the degradation of HSP90 client protein androgen receptor.[18] Celastrol is a triterpene with promising anticancer activity in several cancer models, including prostate cancer, pancreatic cancer, leukemia and melanoma.[19-23] A recent study using a rat mammary carcinosarcoma model (W256 cells) reported that Celastrol not only suppressed tumor cell growth but also inhibited cell migration in vitro; in vivo, Celastrol suppressed trabecular bone loss and reduced osteolytic lesions in tumor-bearing rats.[24] The additional ability of Celastrol to inhibit bone metastasis,[24] as opposed to a potential pro-metastatic effect of 17-AAG,[17] suggests a therapeutic advantage for Celastrol over 17-AAG as an HSP90 inhibitor.

In addition to targeting the proteasome and HSP90, Celastrol has been shown to inhibit NFκB activation by modifying a reactive cysteine on IκB kinase α.[25] Since NFκB signaling has been implicated in providing resistance to apoptosis by upregulating anti-apoptotic factors as well as by regulating bone metastasis and osteoclatogenesis, the ability of Celastrol to inhibit the NFκB pathway significantly adds to its therapeutic value. The ability of Celastrol to react with free thiol groups via its 'Michael Acceptor' (α,β-unsaturated ketone) functionality appears to be important for its biological activity.[26] One potential consequence of thiol reactivity is the induction of oxidative stress by altering the cellular redox balance, which could elevate the levels of reactive oxygen species (ROS). Recent data suggest that elevation of ROS in cancer cells, which already have higher basal ROS as compared to normal cells, may preferentially trigger cell death by further elevating the level of oxidative stress.[27] The HSP90 and proteasome inhibitory properties of Celastrol may further facilitate ROS induction by eliciting an unfolded protein response (UPR) and endoplasmic reticulum (ER) stress.[28] Thus, Celastrol represents a relatively unique pharmacophore that targets HSP90 as well as other functional pathways of relevance to ErbB2-driven oncogenesis.[19,22] Here, we show that Celastrol exhibits relatively selective anticancer activity towards ErbB2-overexpressing breast cancer cells that is dependent on its Michael acceptor functionality, and that Celastrol is strongly synergistic with ErbB2-targeted therapeutic agent Trastuzumab.

Results

Celastrol exhibits potent in vitro and in vivo antitumor activity against ErbB2-overexpressing breast cancer cells. We first evaluated the cytotoxicity of Celastrol towards a panel of ErbB2-overexpressing breast cancer cell lines including SKBr-3, BT-474, 21MT-1 and JIMT-1 (a Trastuzumab-resistant cell line[29]). ErbB2-low breast cancer cell line MCF-7 and immortalized but non-tumorigenic mammary epithelial cell line MCF-10A were also used for comparison. Cytotoxicity profiles (**Fig. 1** and associated Table) clearly showed a higher level of killing of ErbB2-overexperssing cell lines SKBr-3, BT-474, 21MT-1 and JIMT-1 by Celastrol (3- to 12-fold lower IC_{50} values) as compared to ErbB2-low MCF-7 and MCF-10A lines. In view of this selectivity, we examined the efficacy of Celastrol against ErbB2-overexpressing BT-474 cell line in a NOD-SCID xenograft model. Mice bearing implanted tumors were treated with 2 or 4 mg/kg Celastrol based on doses reported in prostate and pancreatic cancer models.[19,22] As Celastrol administration on alternate days induced about 20% loss in body weight (see **Fig. 2A**), the mice were subsequently given Celastrol every third day. At both doses (2 and 4 mg/Kg), Celastrol significantly retarded the rate of tumor growth (**Fig. 2B**) with only modest weight loss (~7% for 2 mg/kg; ~12% for 4 mg/kg versus ~3% for the vehicle control group; **Fig. 2A**). While tumors in vehicle-treated mice grew an average of 25-fold (vs. initial tumor volume), Celastrol-treated mice showed only a ~6-fold or ~4.5-fold increase in tumor volume at 2 or 4 mg/kg Celastrol, respectively. Notably, while four out of ten mice in the group treated at 4 mg/kg Celastrol died (at days 40, 46, 61 and 70), no deaths were observed in the 2 mg/kg treatment group, indicating substantial effectiveness with low toxicity.

Synergistic killing of ErbB2-overexpressing tumor cells by a combination of celastrol with trastuzumab or lapatinib. Given the higher Celastrol-induced cytotoxicity towards ErbB2-overexpressing tumor cell lines, we reasoned that a combination of Celastrol with ErbB2-targeted agents may be additive or synergistic. Thus, we assessed the dose-response of Celastrol alone or in combination with Trastuzumab (**Fig. 3A and B**) or the dual EGFR/ErbB2 kinase inhibitor Lapatinib[1,30] (**Fig. 3C and D**) on the viability of ErbB2-overexpressing breast cancer cell line SKBr-3 (**Fig. 3A–D**). A dramatic reduction in the IC_{50} value of Celastrol (~48-fold; from 130 nM for single drug versus 2.7 nM when combined with 1 μg/ml Trastuzumab) clearly indicated a strong synergy with Trastuzumab (**Fig. 3A and B**). Analyses of Celastrol effects in combination with Lapatinib utilized two distinct formats: (1) increasing concentrations of drugs combined at a fixed 10:1 ratio of Celastrol to Lapatinib; and (2) variable concentrations of Lapatinib with a fixed (50 nM) but sub-optimal concentration of Celastrol. The first experimental format (**Fig. 3C and D**) showed that inclusion of Celastrol reduced the IC_{50} of Lapatinib on SKBr-3 cells from 25 nM to 3.5 nM (a 7-fold reduction). The second experimental format confirmed the synergistic interaction (**Sup. Fig. 1A and B**): the IC_{50} value for Lapatinib in the presence of 50 nM Celastrol was 0.74 nM as opposed to 25 nM when treated as a single drug (a 34-fold reduction). Analysis using the Chou-Talalay method also confirmed the synergistic drug interactions (**Fig. 3B and D**). The synergism was selective for ErbB2-overexpressing cells as similar analyses with ErbB2-low MCF-7 cell line did not show synergism (**Sup. Fig. 2**).

Since Celastrol and 17-AAG both target HSP90 but Celastrol targets additional biological targets[19,20,25,31] some synergism might be expected between these agents. Indeed, treatment of SKBr-3 cells with varying concentrations of Celastrol and 17-AAG (at a fixed ratio of 20:1) showed that IC_{50} for Celastrol in combination with 17-AAG was 78 nM compared to 130 nM when tested alone (~1.7-fold reduction) (**Sup. Fig. 3**); Chou-Talalay analysis supported this mild synergism, as reported earlier in a prostate cancer model.[18] These studies suggest a promising therapeutic potential of Celastrol especially when used in combination with ErbB2-targeted agents where it should be feasible to use relatively low doses that do not produce significant toxicity.

Celastrol induces the ubiquitinylation and lysosomal degradation of ErbB2. As Celastrol reportedly modulates HSP90 function.[18,22,32] We examined if Celastrol, similar to HSP90 inhibitor 17-AAG,[13,33,34] induces the degradation of ErbB2. Similar to the effect of 17-AAG, treatment of ErbB2-overexpressing breast cancer cell lines SKBr-3 and 21MT-1 with Celastrol induced a dose- and time-dependent depletion of ErbB2 protein (**Fig. 4A and B**) as well as other HSP90 client proteins c-Raf and phospho-AKT (**Fig. 4C**). Since a combination of Celastrol and Trastuzumab synergistically inhibited the growth of ErbB2-overexpressing breast cancer cells (**Fig. 3A and B**), we wished to assess if more effective ErbB2 degradation by the combination can partly account for the synergistic effects. However, we did not find substantial differences in the extent of ErbB2 degradation upon treatment with Celastrol plus Trastuzumab as compared to single drug treatment (**Fig. 4D**), unlike our published results with 17-AAG plus Trastuzumab combination.[13] As 17-AAG has been reported to induce a reduction in the levels of phospho-ErbB2 (p-ErbB2) prior to actual depletion of ErbB2 protein,[35] we examined the effects of Celastrol (17-AAG was included for comparison) on p-ErbB2 versus total ErbB2 levels using ErbB2-overexpressing 21MT-1 cells. Consistent with reported findings,[35] 17-AAG induced a rapid (as early as 5 min) reduction in p-ErbB2 levels (**Fig. 4E**). Interestingly, Celastrol treatment also led to a decrease in p-ErbB2 levels before any noticeable reduction in total ErbB2 protein levels. However, the effect of Celastrol on p-ErbB2 was slower compared to that of 17-AAG, yet more sustained.

Consistent with HSP90 inhibitor-induced ErbB2 degradation being preceded by ubiquitinylation,[13,33,34] we observed that Celastrol treatment of 21MT-1 cells induced the ubiquitinylation of ErbB2 (**Fig. 4F**). Accumulation of ubiquitinylated ErbB2 in Celastrol-treated cells even in absence of Lactacystin is consistent with the reported proteasome inhibitory activity of Celastrol;[19] however, unlike Lactacystin, the reported proteasome inhibitory activity of Celastrol appears to be insufficient to block 17-AAG-indued degradation of ErbB2 (**Fig. 4G**).

Using Confocal Immunofluorescence Microscopy (CIM), we established that Celastrol induces the depletion of ErbB2 from

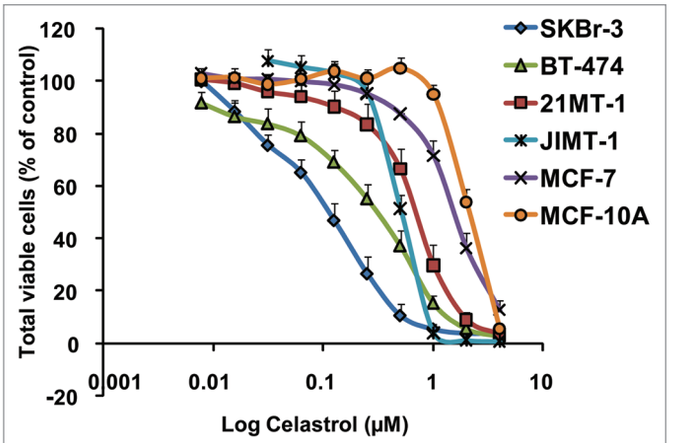

Cell line	IC50 (μM)
SKBr-3	0.13 ± 0.02
BT-474	0.16 ± 0.02
21MT-1	0.53 ± 0.13
JIMT-1	0.48 ± 0.02
MCF-7	1.56 ± 0.24
MCF-10A	1.23 ± 0.47

Figure 1. Sensitivity of various breast cancer cell lines towards Celastrol. The sensitivity of a panel of breast cancer cell lines overexpressing ErbB2 (SKBr-3, BT-474, 21MT-1 and JIMT-1) to Celastrol were evaluated using MTT assay a described in the methods section. For comparison, ErbB2-low expressing cell lines MCF-7 and MCF-10A were also included. The viable cells at the end of treatment were assessed using the MTT dye assay and data represented as % of vehicle control. Shown here are the dose-response curves (mean of three independent experiments run in duplicates) for killing of breast cancer cells with Celastrol. The calculated IC_{50} values are tabulated below.

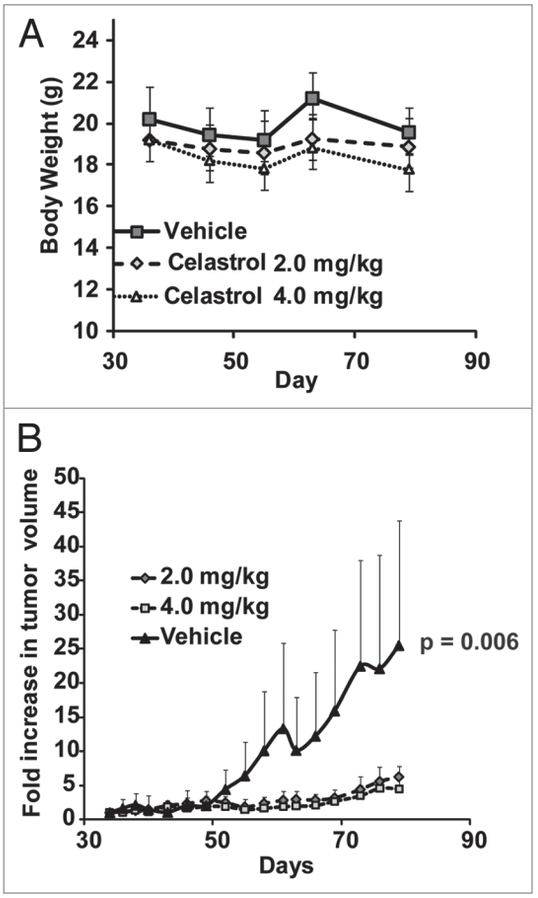

Figure 2. Celastrol retards growth of ErB2-overexpressing breast cancers in xenograft models: NOD-SCID mice with BT-474 tumor xenografts (n = 10 per treatment group) were treated with vehicle control or the indicated doses of Celastrol, as detailed in the experimental section. The change in body weight is shown in (A), whereas (B) compares the increase in tumor volume (relative to the initial tumor volume before drug treatment ±SE) with and without drug treatment. Statistical differences were estimated using Student's t-test (two-tailed; two-sample equal variance).

the cell surface and that the internalized ErbB2 (stained in green) colocalizes (regions with yellow staining) with late endosomal/lysosomal marker LAMP-1 (stained in red) (**Fig. 5**), similar to lysosomal localization of ErbB2 upon 17-AAG treatment.[13] Next, we assessed whether the Michael acceptor group in Celastrol is functionally important in ErbB2 degradation. Pre-treatment of Celastrol with DTT (before adding in cell cultures) or conversion to Dihydrocelastrol (chemical reduction of α,β-unsaturated ketone group to a 'Michael adduct') abrogated the ability of Celastrol to induce ErbB2 degradation (**Fig. 6A**; compare lanes 4 & 8). As anticipated, pretreatment of 17-AAG with DTT had no effect on its ability to induce ErbB2 degradation (**Fig. 6A**; compare lanes 12 & 16). These results indicate that α,β-unsaturated ketone functionality of Celastrol is important for its HSP90 inhibitory activity. Similar to its effects on Celastrol-induced ErbB2 degradation, DTT pretreatment of Celastrol markedly reduced its effect on ErbB2 ubiquitinylation (**Fig. 6B**; compare lane 3 with 7 and lane 4 with 8). The lower levels of ErbB2 in lanes 3 and 7 likely reflect partial Celastrol-induced ErbB2 degradation.

Celastrol induces G_1 cell cycle arrest and apoptosis. Given the importance of the Michael acceptor functionality in Celastrol-induced ErbB2 ubiquitinylation and degradation, we also assessed its importance in Celastrol-induced cytotoxicity. Similar to 17-AAG,[13,36] treatment of 21MT1 cells with Celastrol (1 μM) induced a pronounced G_1 cell cycle arrest (**Fig. 7A**). Higher concentrations (2 μM) induced a significant degree of apoptosis as seen by an increase in the proportion of cells in the sub-G_1 fraction (**Fig. 7B**), cells positive for Annexin V staining (**Fig. 7C**) and the level of PARP cleavage (**Fig. 7D**). Abrogation of the 'Michael acceptor' functionality (Celastrol vs. Dihydrocelastrol) markedly reduced the ability of Celastrol to induce apoptosis (**Fig. 7C**).

To further assess the importance of the Michael acceptor in the bioactivity of Celastrol, we assessed the ability of Celastrol to induce vacuolation, an apparent result of Celatsrol-induced ER-stress and unfolded protein response (UPR).[37] Celastrol treatment (4 μM) of SKBr3 (**Sup. Fig. 4**) or 21MT1 (**Fig. 8A**) cells for 4 h resulted in the formation of large vacuoles; pre-treatment of Celastrol with DTT led to a substantial reduction in their appearance. Similar results were seen with Dihydrocelastrol (**Fig. 8A**). Reduction in the proportion of cells with rounded morphology (dying cells) also indicated a delay in the induction of cell death with Dihydrocelastrol vs. Celastrol (**Fig. 8A and Sup. Fig. 5**), confirming results using Annexin-V staining (**Fig. 7C**). Analysis of samples used in **Figure 8A** confirmed that Dihydrocelastrol also did not induce ErbB2 degradation (**Fig. 8B**). Finally, an MTT assay confirmed the reduced antiproliferative activity of Dihydrocelastrol compared to Celastrol against SKBr-3 and BT-474 cells (**Fig. 8C and D**). Collectively, these results indicate that the anticancer activity of Celastrol towards ErbB2-overexpressing breast cancer cells is dependent on it Michael acceptor functionality.

Role of oxidative stress and reactive oxygen species (ROS) generation in the bioactivity of celastrol. Cancer cells are under high oxidative stress and generate higher levels of ROS; however, upregulation of redox buffering mechanisms allows them to grow despite elevated ROS levels.[38] Given the importance of the Michael acceptor functionality for the biological activity of Celastrol, and the propensity of this group to covalently react with cellular free thiols (on reduced Glutathione and redox-balancing enzymes),[26] we asked if higher Celastrol sensitivity of ErbB2-overexpressing breast cancer cell lines reflects elevation of ROS levels; in this regard, Celastrol might function by further increasing the already elevated oxidative stress levels beyond a threshold that is compatible with cell viability, as has been proposed recently.[27] Consistent with this scenario, ErbB2 overexpression is known to increase ROS levels via the activation of Rac1/NADPH oxidase, PI3K/AKT and other pathways.[39,40] Indeed, overexpression of exogenous ErbB2 in ErbB2-low BT20 or MCF-10A (**Fig. 9A and B**) cell lines increased the basal ROS levels. Furthermore, analysis of ROS levels in the panel of cell lines used to assess the cytotoxicity of Celastrol (**Fig. 1** and associated table), indicated higher levels of basal ROS (**Fig. 9C**) in cell lines

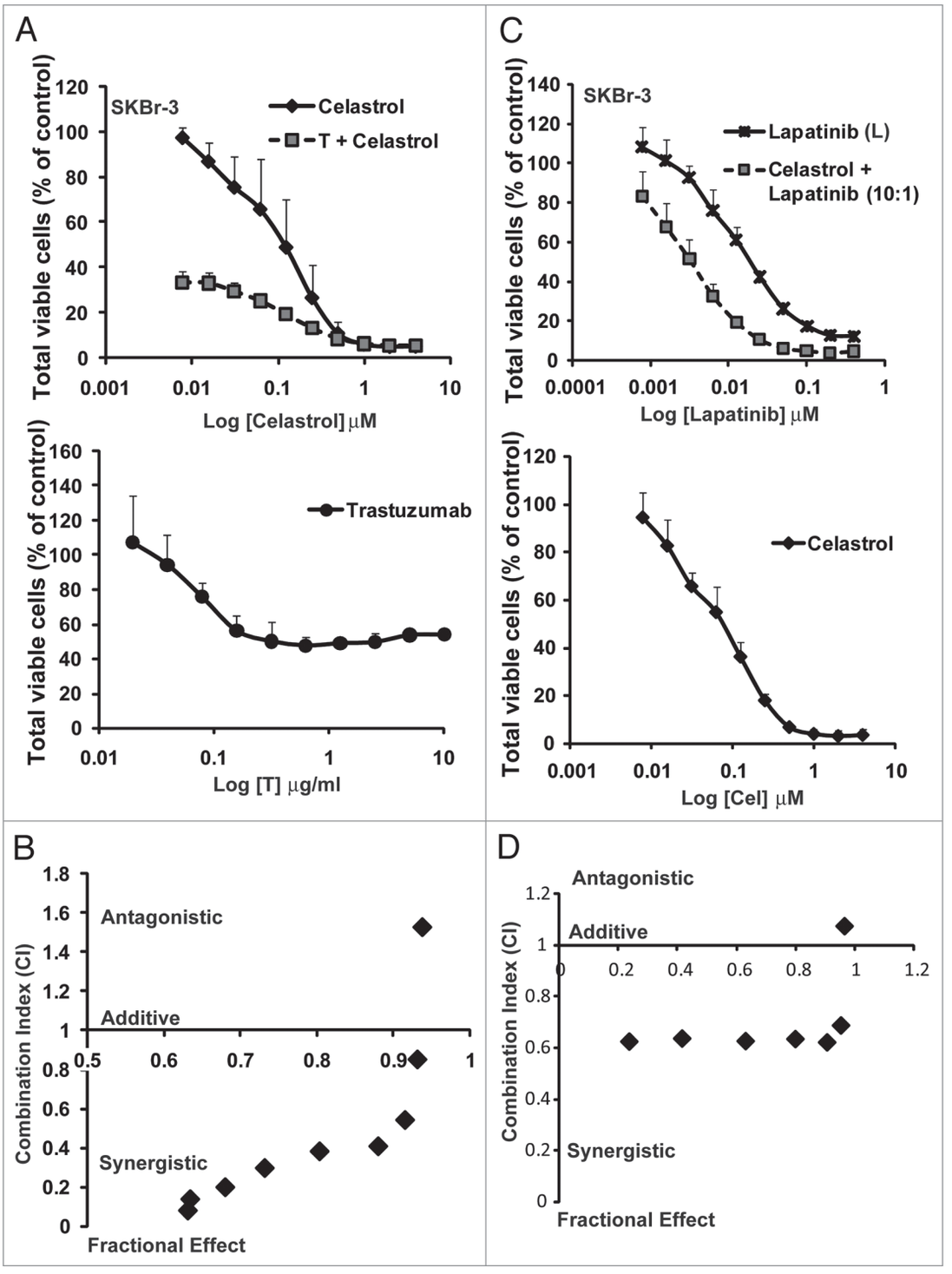

Figure 3. Celastrol in combination with ErbB2-targeted drugs, Trastuzumab and Lapatinib, synergistically induces cytotoxicity ErbB2-overexpressing breast cancer cells: SKBr-3 cells were treated with Celastrol as a single drug or in combination with Trastuzumab or Lapatinib as described in the methods section. The viable cells at the end of treatment were assessed using the MTT dye assay and data represented as % of vehicle control. Shown here is the comparison of cytotoxicity of single drug treatments or combination with Trastuzumab (A) or Lapatinib (C), showing efficacy of combinatorial treatment over single drugs. (A) The IC_{50} for Celastrol alone was 0.13 ± 0.02 μM; whereas it was 0.0027 ± 0.001 μM when combined with Trastuzumab at 1 μg/ml. The % cell viability for SKBr-3 treated with Trastuzumab alone at this concentration was 51.4 ± 7.7. (C) The IC_{50} for Lapatinib was 25.5 ± 2.1 nM as a single drug versus 3.5 ± 1.6 nM when combined with Celastrol. Also shown are Chou-Talalay analyses for Celastrol plus Trastuzumab (B) or Celastrol plus Lapatinib (D) combination. Combination index (CI) <1 indicates synergy; CI ~ 1 indicates additive effects; CI >1 indicates antagonism.

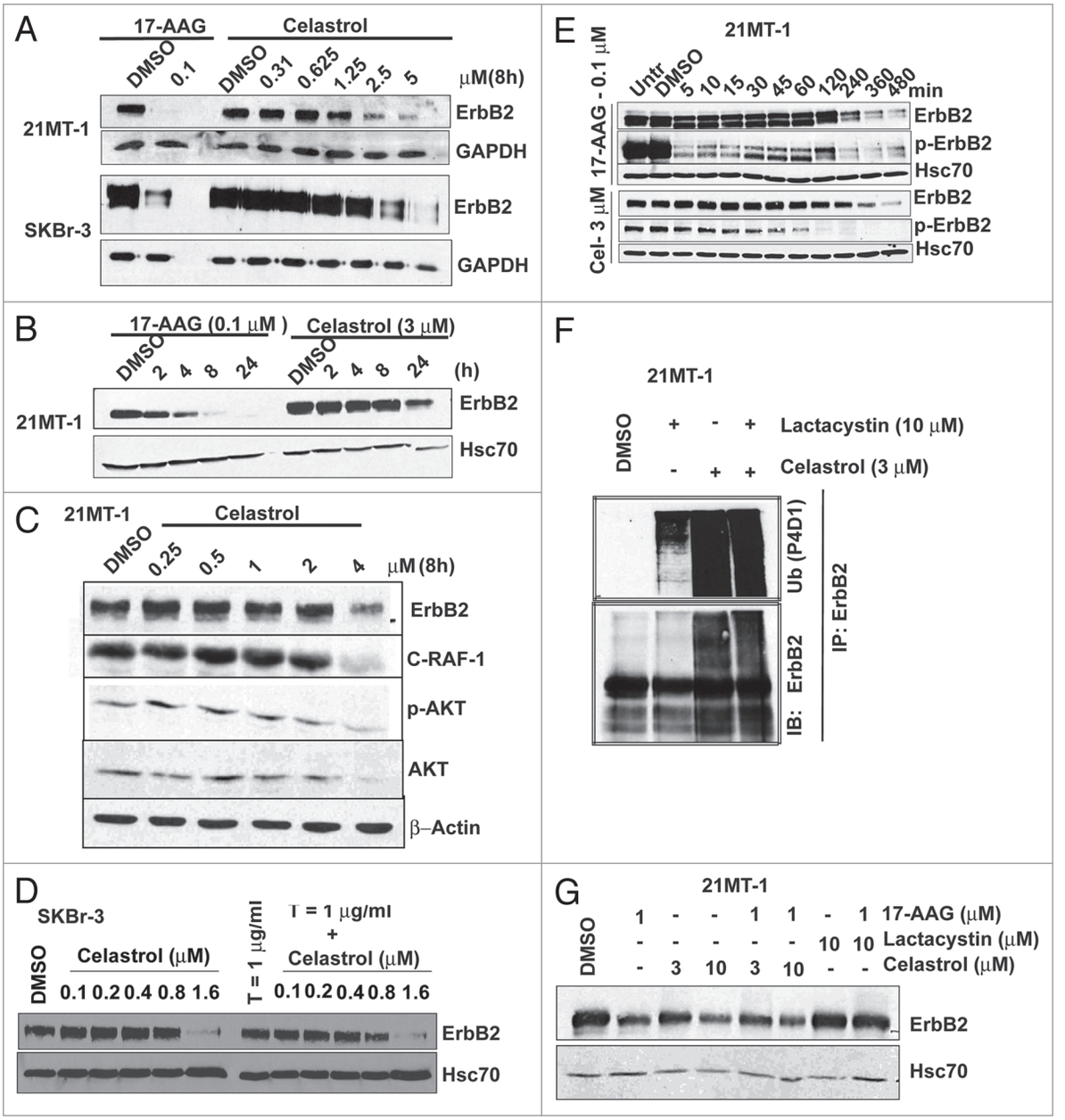

Figure 4. Celastrol induces the ubiquitinylation and degradation of ErbB2 and other HSP90 client proteins: (A) ErbB2-overexpressing breast cancer cell lines 21MT-1 and SKBr-3 were treated with 17-AAG or Celastrol at the indicated concentrations for 8 h. Shown here is the decrease in ErbB2-levels after treatment. GAPDH was used as a loading control. (B) 21MT-1 cells were treated with the 17-AAG (0.1 μM) or Celastrol (3 μM) for indicated the indicated time periods. Shown here is the comparison of the kinetics of Celastrol-induced ErbB2 degradation in 21MT-1 cells with that induced by 17-AAG, at the indicated concentrations. (C) 21MT-1 cells were treated with the indicated concentrations of Celastrol for 8 h. The effect of Celastrol on other HSP90 client proteins is shown here. (D) SKBr-3 cells were treated with the indicated concentrations of Celastrol (as a single drug) or in combination with Trastuzumab at 1 μg/ml for 48 h. Equal amount of protein from cell lysates were analyzed for changes in ErbB2 levels. Hsc70 was used as a loading control. (E) 21MT-1 cells were treated with 17-AAG or Celastrol at the indicated concentrations for the time periods shown. Cell lysates were analyzed for total ErbB2 and p-ErbB2 levels. Hsc70 is shown as a loading control. (F) 21MT-1 cells were treated (as indicated) with Lactacystin (Lct) or Celastrol (Cel) or Lct plus Cel, for a total of 4 h. Cell lysates in RIPA buffer were used for anti-ErbB2 immuno-precipitation and sequentially immunoblotted for Ub and ErbB2. (G) 21MT-1 cells were pre-treated for 1 h with Lactacystin or Celastrol, at the indicated concentrations followed by treatment with 17-AAG for an additional 3 h. Cell lysates were analyzed by immunoblotting for ErbB2 and Hsc70 (loading control).

with higher sensitivity to Celastrol. Notably, Celastrol treatment of SKBr-3 cells further increased the ROS levels (**Fig. 9D**).

To assess the relative contribution of ROS modulation versus inhibition of other targets in the biological activity of Celastrol, we assessed whether anti-oxidants can protect ErbB2-overexpressing breast cancer cells from cytotoxic effects of Celastrol. Treatment of SKBr-3 cells with Celastrol (4 μM) in the presence of a 500-fold molar excess of known anti-oxidants, including N-acetyl

cysteine (NAC) or Trolox® (a water soluble derivative of Vitamin E) delayed the induction of cell death by Celastrol although these agents did not abrogate the eventual cytotoxicity, as assessed by cell morphology and confirmed by Annexin V assay (**Fig. 10 and Suppl. Fig. 6**), suggesting that multiple activities (against HSP90, proteasome and NFκB pathway and others) of Celastrol contribute to its overall cytotoxic activity.

Discussion

Targeted therapy of ErbB2-overexpressing breast cancers with Trastuzumab represents a significant advance; however, de novo as well as acquired resistance to Trastuzumab necessitate additional therapeutic approaches that can work in concert with ErbB2-targeted agents. Agents that target multiple signaling nodes and/or cellular pathways selectively driven by overexpressed ErbB2 are particularly compelling as their combination with ErbB2-targeted agents can lead to synergistic therapeutic effects, and help overcome or reduce the likelihood of resistance. Indeed, as we have recently shown, abrogation of the protective role of molecular chaperone HSP90 towards ErbB2 and its downstream signaling components allows synergistic and relatively selective killing of ErbB2-overexpressing breast cancer cells.[13] Here, we demonstrate that a natural triterpene Celastrol, which possesses HSP90 inhibitory activity but also additional biological properties, has high selectivity against ErbB2-overexpressing breast cancers, including the Trastuzumab-resistant cell line model JIMT-1.[29] Since ErbB2 is a major HSP90 client protein and HSP90 inhibitors such as 17-AAG show relatively high selectivity towards ErbB2-overexpressing cancer cells, we speculate that high selectivity of Celastrol towards ErbB2-overexpressing breast cancer cell lines is also partly due to its ability to target HSP90. Consistent with the HSP90 inhibitory activity of Celastrol deduced from its ability to induce a gene expression profile overlapping with that of 17-AAG[18] and its ability to activate the heat shock factor,[41] it induced the ubiquitinylation and degradation of ErbB2 (**Figs. 4F and 6B**) via lysosomal targeting (**Fig. 5**) reminiscent of 17-AAG effects. Celastrol also induced rapid depletion of other HSP90 client proteins (**Fig. 4C**) and depleted phospho-ErbB2 prior to ErbB2 degradation (**Fig. 4E**), as also seen with 17-AAG.[35] It is notable however that the mechanism(s) by which Celastrol influences ErbB2 activity and stability differs from that of other HSP90 inhibitors such as 17-AAG. Celastrol activity appears to be critically dependent on its Michael acceptor functionality (**Figs. 6 and 8**) consistent with findings that heat shock factor activation by Celastrol involves its ability to interact with thiols.[26] Unlike 17-AAG which competes with ATP for binding and

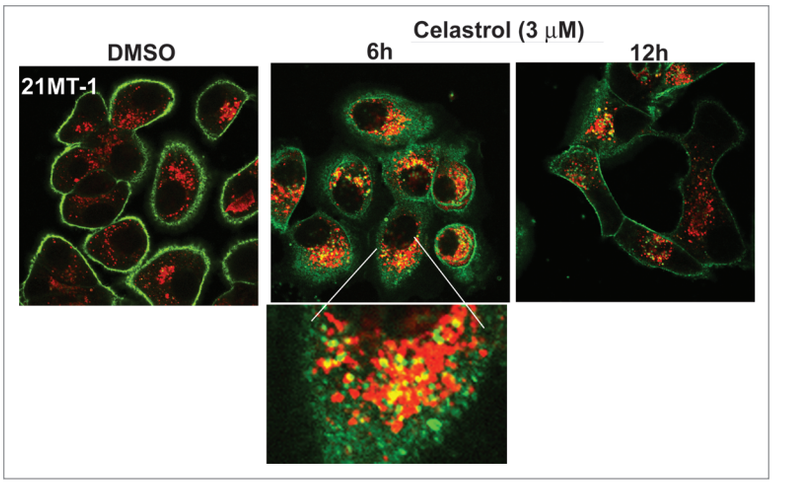

Figure 5. Celastrol induces lysosomal degradation of ErbB2: 21MT-1 cells, grown on coverslips were treated with the indicated concentrations of Celastrol for the indicated time periods. The coverslips, after treatment, were immunostained for ErbB2 and LAMP-1. ErbB2 staining is in green and LAMP-1 in red; colocalized regions are seen as yellow.

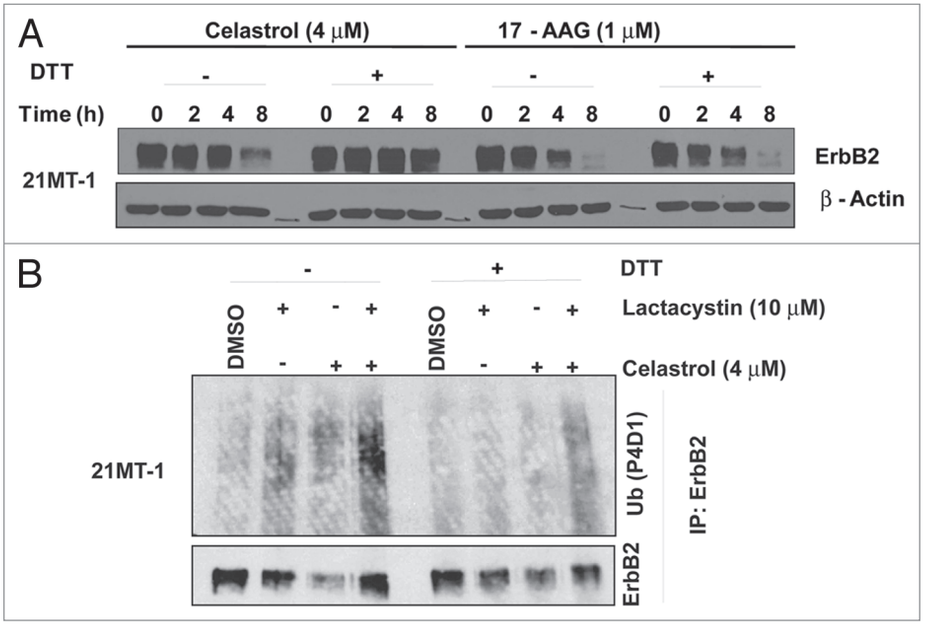

Figure 6. The role of Michael acceptor moiety in Celastrol towards its activity to destabilize ErbB2: (A) 21MT-1 cells were treated with Celastrol (4 μM) or 17-AAG (1 μM) (from a 100x stock that was left untreated or pre-treated with DTT) for the indicated time points. Cell lysates were analyzed by immunoblotting for ErbB2 and β-actin (used as a loading control). (B) 21MT-1 cells were incubated (as indicated) for 3 h with Celastrol (with or without pre-treatment with DTT) in absence or presence of Lactacystin (cells pre-treated for 1 h). Anti-ErbB2 immunoprecipitates were sequentially immunoblotted for Ub and ErbB2.

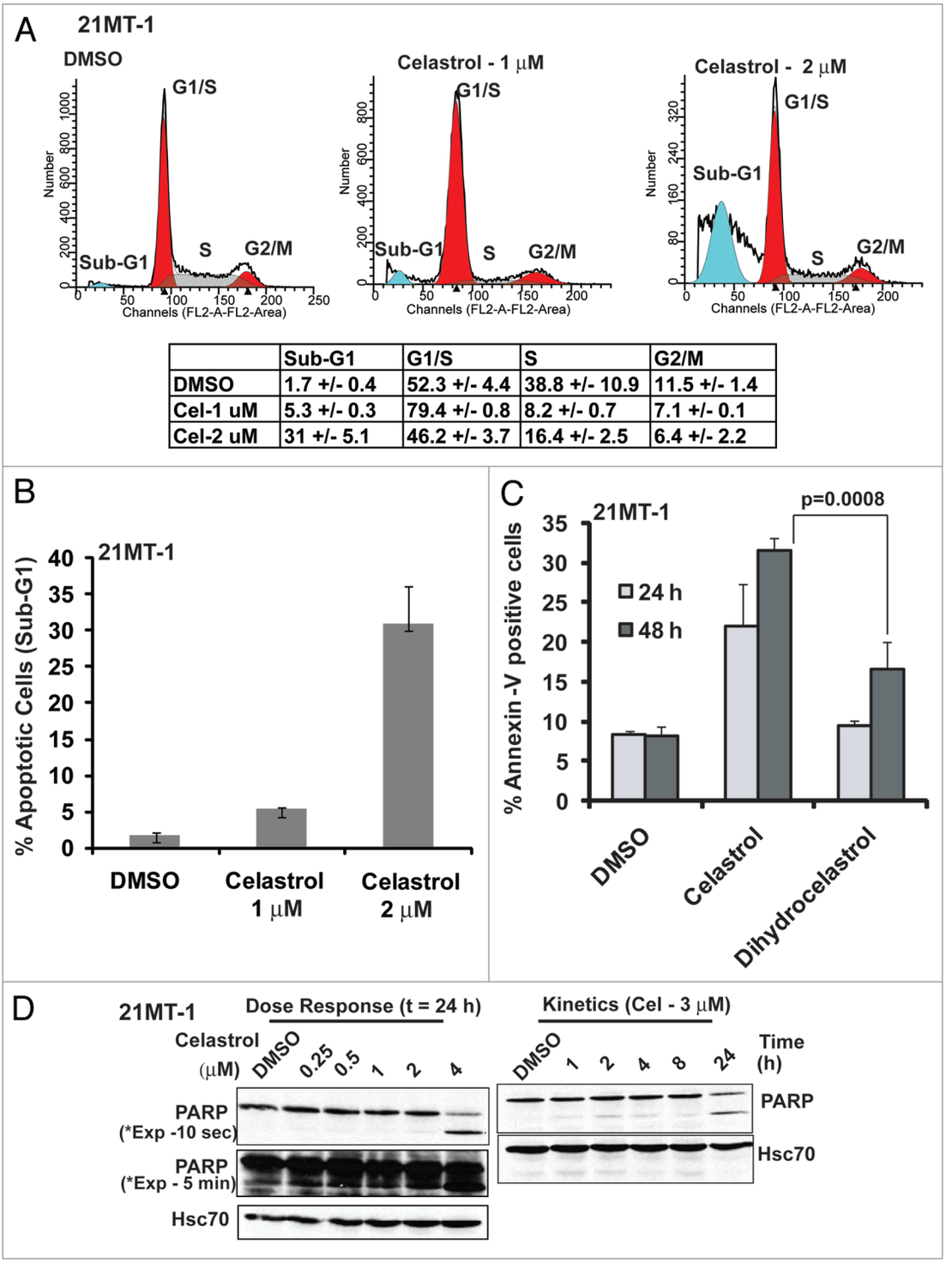

	Sub-G1	G1/S	S	G2/M
DMSO	1.7 +/- 0.4	52.3 +/- 4.4	38.8 +/- 10.9	11.5 +/- 1.4
Cel-1 uM	5.3 +/- 0.3	79.4 +/- 0.8	8.2 +/- 0.7	7.1 +/- 0.1
Cel-2 uM	31 +/- 5.1	46.2 +/- 3.7	16.4 +/- 2.5	6.4 +/- 2.2

Figure 7. Celastrol induces G_1-arrest and apoptosis in ErbB2-overexpressing breast cancer cells: 21MT-1 cells were treated with the indicated concentrations of Celastrol for 24 h. Samples were prepared in triplicate wells. Following treatment, the samples were subjected to cell cycle analysis using FACS, as described in materials and methods. (A) Representative cell cycle profiles of DMSO-treated or Celastrol-treated 21MT-1 cells are shown and a table is presented detailing the % (±SD) of cells in various phases of cell cycle. (B) Comparison of % apoptotic cells in sub-G_1 fraction analyzed from cell cycle analysis plots; (C) 21MT-1 cells were treated with 2 μM Celastrol or Dihydrocelastrol for 24 or 48 h and analyzed for apoptosis by Annexin-V staining using FACS. Propidium Iodide (PI) was included to identify dead versus dying population of cells. Shown here is the % Annexin-V positive/PI negative population (apoptotic cells); (D) 21MT-1 cells were treated at the indicated concentrations of Celastrol and for the indicated time periods. Cell lysates were analyzed for intact and cleaved PARP by immunoblotting. Hsc70 is shown as a loading control.

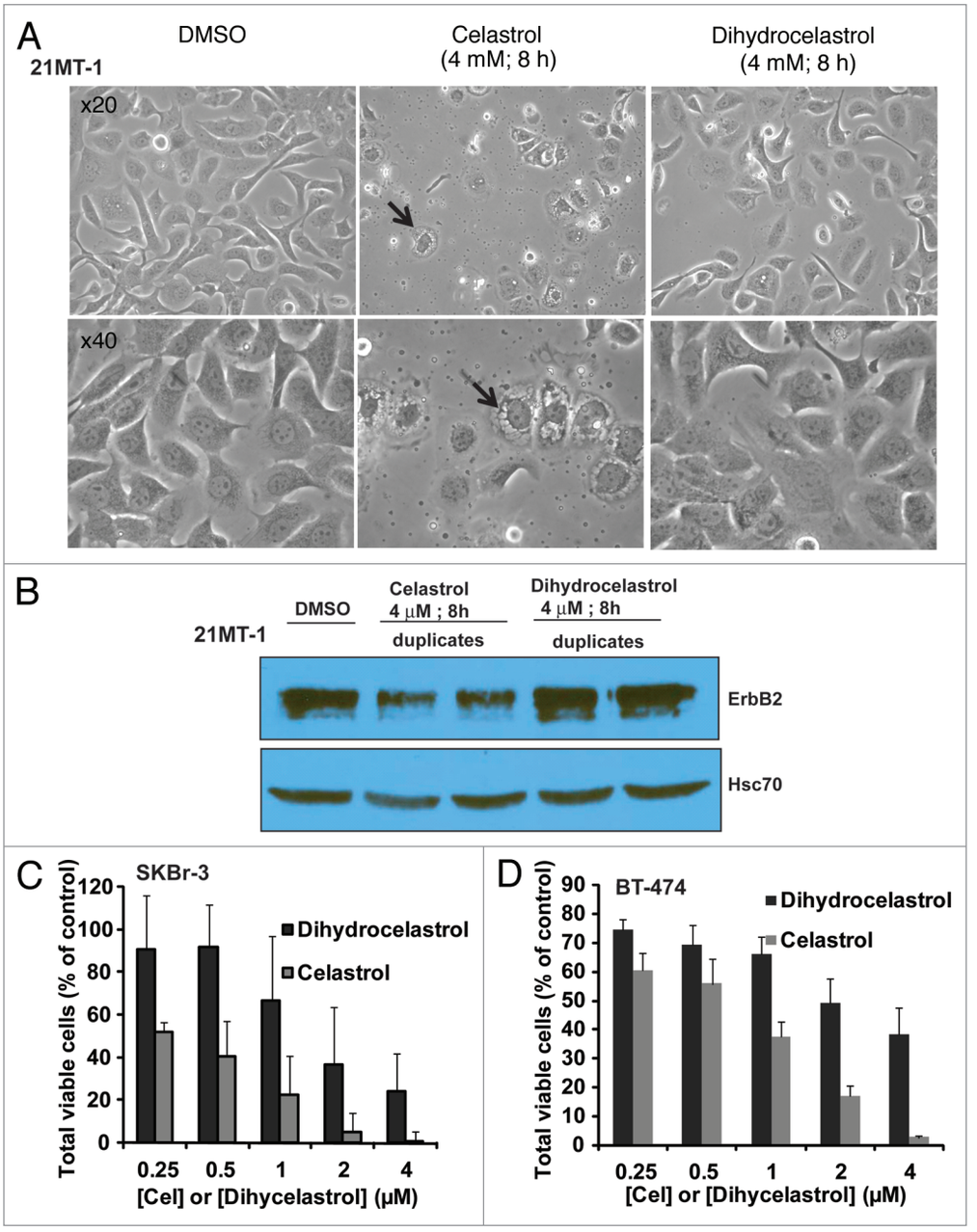

Figure 8. The requirement of 'Michael acceptor' functionality in the bioactivity of Celastrol: (A) Effect of reduction of the α,β-unsaturated carbonyl group by sodium borohydride on Celastrol- or Dihydrocelastrol-induced cell death in SKBr-3 cells. Cells were incubated with DMSO or indicated concentrations of Celastrol or Dihydrocelastrol. Photographs were acquired using a bright field microscope with a x20 or x40 objective. (B) Comparison of Celastrol and Dihydrocelastrol for induction of ErbB2 degradation in 21MT-1 cells. Samples from the experiment shown in (A) were analyzed for ErbB2 degradation using immunoblotting. Hsc70 is shown as a loading control. (C and D) Comparison of the effects of Celastrol and Dihydrocelastrol on SKBr-3 (C) or BT-474 (D) cell lines as measured in an MTT assay. Cells were treated with the indicated concentrations of Celastrol of Dihydrocelastrol for 3 days. Cell growth was measured by MTT assay.

inhibits the ATPase activity of HSP90,[42] Celastrol appears to inhibit the function of HSP90 by disrupting its interaction with co-chaperone Cdc37.[22] The disruption of HSP90-CDC37 interaction appears to involve the ability of Celastrol to modify free thiols and form Michael adducts with CDC37,[32] consistent with our results that Celastrol-induced ErbB2 ubiquitinylation and degradation as well as its early cytotoxic effects are dependent on Michael acceptor functionality. However, while the HSP90 inhibitory activity of Celastrol is likely to be important, other activities such as NFκB inhibition,[20,25] are also likely to be important as these pathways are activated downstream of ErbB2. The involvement of such pathways, which control the balance between pro- and anti-apoptotic factors, cell survival and proliferation, may also help explain the relative differences in the

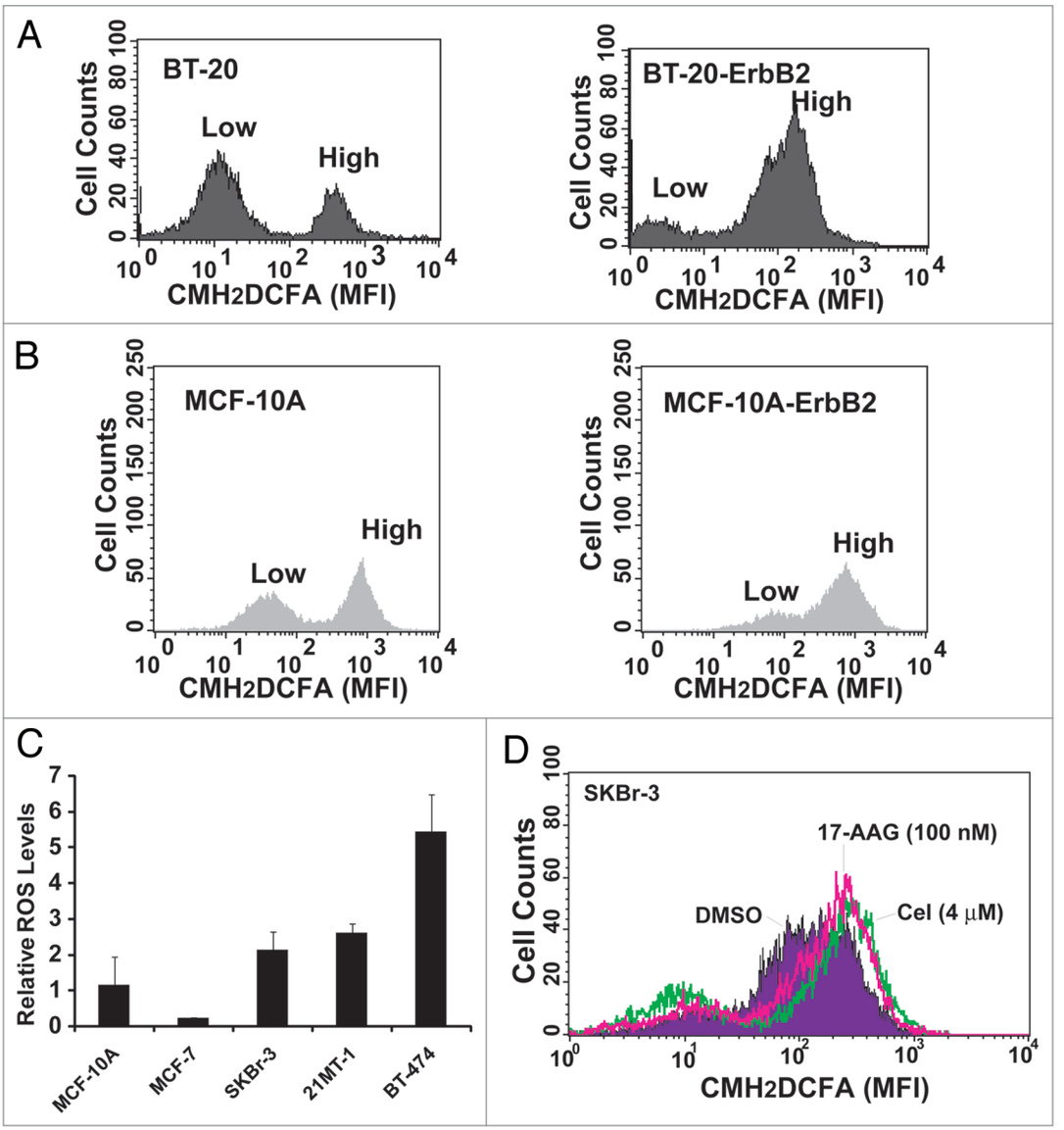

Figure 9. Correlation between ErbB2 expression and basal ROS levels: Parental BT-20 (A) or MCF-10A (B) cell lines and their ErbB2-overexpressing derivatives were analyzed for basal ROS levels by loading with 5 μM CM-H2DCFDA followed by flow cytometry. Typically two peaks are seen in the FACS profile, representing distinct population of cells with low and high ROS. Note an increase in the brighter peak upon ErbB2 overexpression. (C) Comparison of basal ROS levels among breast cancer cell lines. Cells were grown for 48 h, trypsinized and stained with CM-H_2DCFDA. Each cell line was analyzed in triplicates. The relative ROS levels are expressed as a ratio of cells with high ROS to low ROS, as analyzed from the two peaks (seen in A and B). (D) Effect of Celastrol or 17-AAG on basal ROS levels in SKBr-3 cell line. Cells treated with Celastrol or 17-AAG at the indicated concentrations for 4 h, following by analysis of ROS levels using flow cytometry after CM-H_2DCFDA loading.

sensitivity of various breast cancer cell lines with comparable ErbB2 overexpression; for example, SKBr-3 and BT-474 showed a substantially higher sensitivity to Celastrol (IC_{50} of ~0.13 and 0.16 respectively; **Fig. 1**) compared to 21MT-1 and JIMT-1 (IC_{50} of ~0.53 and 0.48 respectively; **Fig. 1**).

Given the ability of the Michael acceptor group to react with cellular thiols, we also considered the potential role of ROS generation in the antitumor activity of Celastrol. The ability of Celastrol to alter cellular redox balance and to increase ROS levels may further account for its ErbB2 selectivity. In this context, ErbB2 is known to increase basal ROS levels by activating PI3K/Akt and Rac1 pathways.[40,43-45] Stable overexpression of ErbB2 in ErbB2-low breast cancer (BT-20) and non-tumorigenic (MCF-10A) cell lines indeed increased basal ROS levels (**Fig. 9A and B**). Furthermore, Celastrol sensitivity in a panel of ErbB2-overexpressing cell lines correlated with high levels of basal ROS (**Fig. 9C**). These findings, together with the delay in Celastrol-induced cell killing by antioxidants (**Fig. 10**) are consistent with the idea that elevation of ROS contributes to cytotoxic activity of Celastrol. However, ROS induction alone does not appear to mediate Celastrol-induced cytotoxicity as delayed cell killing could still be observed in the presence of antioxidants. It is noteworthy that recent studies in a

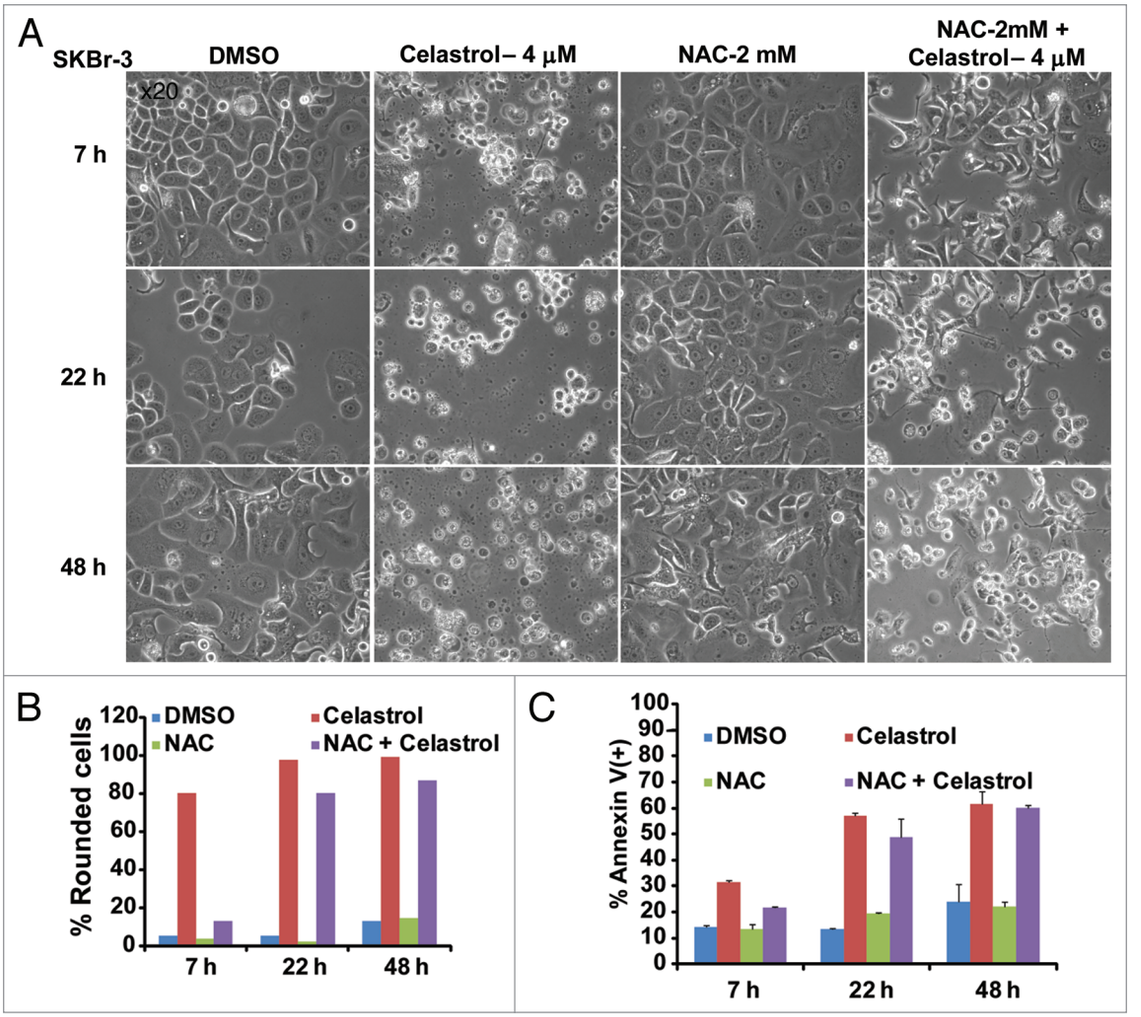

Figure 10. The anti-oxidant N-acetyl Cysteine delays although it does not abrogate Celastrol-induced cell death. (A) Effect of N-acetyl Cysteine (NAC) on Celastrol-induced cytotoxicity in SKBr-3 cell line. Cells were treated with the indicated concentrations of Celastrol with or without a 500-fold excess of NAC. Changes in cell morphology were recorded at the indicated time points under a bright field microscope using a x20 objective. (B) Quantification of the cytotoxic effect of Celastrol and protective effect of NAC analyzed by counting rounded cells. Celastrol induced cell death was evaluated by counting the number of rounded versus flat/attached cells for each treatment condition. The % of cells with rounded morphology (in relation to total cells counted) is shown. (C) Quantification of the cytotoxic effect of Celastrol and protective effect of NAC analyzed using Annexin-V staining. Cells were treated with Celastrol or Celastrol plus NAC for the indicated time points and analyzed for Annexin V staining using flow cytometry.

leukemia model showed that a pro-oxidant Fenretinide induced a relatively transient increase in ROS generation followed by activation of anti-oxidant mechanisms;[46] in this regard, Celastrol-induced rapid ROS generation and delayed ROS-independent cytotoxicity could represent advantageous traits to exploit with the use of Celastrol as an anticancer agent.

How ROS induction might contribute to anticancer activity of Celastrol will need further elucidation. Recent studies have indicated that higher levels of ROS in tumor cells are counterbalanced by the induction of anti-oxidant defenses that involve the titration of ROS as well as counteracting their effects on cell physiology. However, this adaptation has been suggested as an "Achilles' heel" in cancer cells as further elevation in ROS could tip the balance towards tumor cell killing while lower ROS levels in normal cells ensure that ROS levels do nor rise to toxic levels and thus allow their survival.[27,43] Notably, overexpression of ErbB2 in ErbB2-low cells elevated ROS levels (**Fig. 9A and B**); furthermore, PI3K/AKT and Rac pathways which are known to be triggered by ErbB2 can also elevate ROS levels.[40,43-45] Thus, agents that elevate cellular ROS levels may prove useful to enhance the effectiveness of ErbB2-targeted therapeutics (such as Trastuzumab). In this regard, targeting of proteotoxic and oxidative stress pathways has been suggested for selective killing of cancer cells,[47] and proteasome and HSP90 inhibitors can induce proteotoxic stress.[48-52] Indeed, treatment of SKBr-3 cells with 17-AAG also led to increase in ROS levels (**Fig. 9D**).

Celastrol, as a single drug, demonstrated potent antitumor activity and high selectivity against ErbB2-overexpressing breast cancer cells in vitro and in vivo. Our rationale to investigate the potential synergism of Celastrol with Trastuzumab was based on its previously demonstrated antitumor activity in other models,[19-23] and its known ability to target HSP90 for

inhibition. Based on our reported studies on the synergistic effects of 17-AAG plus Trastuzumab combination,[13] we predicted that Celastrol in combination with Trastuzumab will also be synergistic. Indeed, this is the case. However, unlike 17AAG and Trastuzumab, Celastrol and Trastuzumab combination did not appear to induce substantially more ErbB2 degradation (**Fig. 4D**). Thus, the mechanism of biological synergy between Celastrol and Trastuzumab is likely to involve downstream factors. Since Celastrol inhibits HSP90, proteasome and the NFκB pathway, and can induce ROS, multiple mechanisms may contribute to the observed biological synergy between Celastrol and Trastuzumab or Lapatinib. The ability of Celastrol to inhibit the NFκB pathway, which is known to be activated by ErbB2 in breast cancers,[20,25] could enhance Trastuzumab activity by suppressing NFκB-mediated anti-apoptotic signaling since combination of NFκB inhibition with a specific peptide synergized with Trastuzumab in ErbB2-overexpressing breast cancer models.[53] Inhibition of NFκB pathway by Celastrol may also contribute to synergy between Celastrol and Lapatinib (**Fig. 3**) as NFκB pathway has been implicated in resistance to the Lapatinib and RNAi based suppression of RelA restored Lapatinib sensitivity.[54] Future studies should help test these ideas. Our findings that Celastrol is strongly synergistic with ErbB2-targeted therapeutics, Trastuzumab and Lapatinib (which are both in clinical use) should help mitigate concerns about the toxicity we observed with the use of Celastrol as a single agent to treat mice bearing xenotransplanted ErbB2-overexpressing tumors. While Celastrol showed potent antitumor activity, some dose-dependent loss of weight (7 or 12% with 2 mg/Kg and 4 mg/Kg doses) (**Fig. 2A**) was noted. This modestly higher level of weight loss in Celastrol-treated mice as compared to vehicle treatment group, together with loss of animals in the group treated with the higher dose, suggests a certain level of toxicity at the doses tested. While the basis of this toxicity (e.g., reduced food intake vs. other effects) needs to be explored further, it is important to point out that a strong antitumor effect was observed even with the lowest dose tested, which showed no deaths among treated animals and produced minimal weight loss. More importantly, since we do not envision the use of Celastrol as a single agent in the clinic but rather in combination with ErbB2-targeted therapeutic agents, the synergism with Trastuzumab and Lapatinib seen in our in vitro studies should allow the use of substantially lower doses of Celastrol and help avoid any significant toxicity.

In conclusion, our studies show that natural triterpene Celastrol, possesses selective activity against ErbB2-overexpressing breast cancer cells that allows synergistic combination of Celastrol with ErbB2-targeted therapeutics. One component of Celastrol activity appears to be related to its Michael acceptor functionality-dependent ROS generation suggesting that targeting of ROS levels together with ErbB2-targeted agents should be investigated.

Materials and Methods

Cell culture. SKBr-3, BT-474, MCF-7, BT-20 and MCF-10A cell lines (ATCC) and were maintained as previously described.[13] The ErbB2-overexpressing breast cancer cell line 21MT-1 was established by Band et al.[55] JIMT-1cell line was from German Collection of Microorganisms and Cell Cultures (DSMZ) and maintained in complete DMEM.

Antibodies and other reagents. The primary antibodies (Ab) used for this study and the conditions of their use are described in **Supplemental Table 1.** Trastuzumab (Herceptin™) was obtained through Evanston Northwestern Healthcare Pharmacy, while 17-AAG was purchased either from Biomol International (Plymouth, PA USA) or from ChemieTek (Indianapolis, IN). Lapatinib for this study was also from ChemieTek (Indianapolis, IN). Celastrol used in our initial studies was provided as a kind gift by Dr. Richard Silverman (Department of Chemistry, Northwestern University, Evanston, IL) and subsequently purchased from PayPay (ππ) Technologies, (Guangdong, China). Dihydrocelastrol was prepared using sodium borohydride reduction as described.[25] The purified product was characterized by NMR spectroscopy. For DTT-pretreatment, Celastrol (400 μM) or 17-AAG (100 μM) was pre-treated (or left untreated) with 100-fold excess of DTT overnight before using as stocks for degradation experiments. Cremophor EL was obtained from BASF Corp.

Confocal immunofluorescence microscopy (CIM), immunoprecipitation (IP) and western blotting (WB). CIM, IPs and IBs were carried out as described previously.[13,56]

Cytotoxicity assays and analysis of drug synergy. Measurement of cytotoxicity using the MTT assay and the experimental design to assess pharmacological interactions has been previously described.[13] Single drug treatments included a serial 2-fold dilution of Celastrol (4 to 0.008 μM), 17-AAG (200 to 0.19 nM), Trastuzumab (5-0.01 μg/ml) or Lapatinib (400 to 0.7 nM). Drug combinations included serial dilutions at fixed ratios: 20:1 for Celastrol plus 17-AAG and 10:1 for Celastrol plus Lapatinib. Trastuzumab plus Celastrol combination included variable Celastrol (4 to 0.008 μM) and fixed Trastuzumab (1 μg/ml) concentrations. Controls included untreated and DMSO-treated cells.

Tumor xenograft models. Four to six week old female NOD-SCID mice (Charles River laboratories) received sub-cutaneous 17β-estradiol pellet (0.72 mg/day; Innovative Research of America, Sarasota, Fl), 2 weeks prior to injection of 5 x 10^6 BT-474 cells resuspended in 4% Matrigel (BD biosciences). Once tumors reached a size of ~30–100 mm^3 (4–6 mm in dimension) (day 34 after cell implantation), the animals were randomized into groups of 10 for treatment with: (a) Vehicle; (b) Celastrol-2 mg/kg and (c) Celastrol-4 mg/kg. Stocks of Celastrol (10 mg/ml in a Cremophor formulation-20% Cremophor EL, 30% propylene glycol, 50% ethanol) were diluted 1:12.5 in saline for injections. Control vehicle was prepared by similarly diluting the solvent into saline. Mice received Celastrol or vehicle injections every other day during the first week and every three days thereafter. Tumor volumes were calculated as: ½ larger diameter x (smaller diameter)^2.[57] Mice were monitored for toxicity everyday and followed until the tumor volume reached 1,000 mm^3. After completion of the studies animals were euthanized using CO_2. All procedures were performed according to Institutional Animal Care and Use Committee guidelines.

ROS measurements. ROS levels were analyzed using 5-(and-6)-chloromethyl-2'-7'-dichlorodihydrofluorescein diacetate acetyl ester (CM-H_2DCFDA) (Invitrogen) according to the manufacturer's protocol and analyzed by flow cytometry after gating on live cells (based on forward and side scatter).

Cell cycle analysis and apoptosis assays. Cell cycle distribution using FACS analysis of propidium iodide (PI)-stained cells and assessment of apoptotic cell population in sub-G_1 fraction used standard protocols. Apoptosis was also assessed by binding of Alexafluor™-488 conjugated Annexin-V (Invitrogen) done according to the manufacturer's instructions and by monitoring PARP cleavage by western blotting.

Acknowledgements

This work was supported by: the NIH (Grants CA116552, CA99163, CA87986 and CA105489 to H.B., and CA94143 and CA96844 to V.B.); DOD Breast Cancer Research Grants (DAMD W81XWH-07-1-0351 to V.B.); CA127239 to (A.N.); Nebraska Department of Health and Human Services (LB-506 grant to S.M.R.); and Nebraska Center for Nanomedicine-Center for Biomedical Research Excellence (NCN-COBRE; seed grant to S.M.R.). T.A.B. was a trainee under an NCI Cancer Biology Training Grant (T32 CA 009476) and is a Susan G. Komen Foundation post-doctoral fellow (KG091363). The Core facilities used here were supported by the Nebraska Research Initiative and the NCI Cancer Center Core Support Grant 5 P30 CA036727 to UNMC-Eppley Cancer Center. We thank Dr. Brian Druker for 4G10 antibody, Dr. Richard Silverman for initial gift of Celastrol, and members of the Band Laboratories for helpful discussions.

Note

Supplemental materials can be found at:
http://www.landesbioscience.com/journals/cbt/article/13959

References

1. Browne BC, O'Brien N, Duffy MJ, Crown J, O'Donovan N. HER-2 signaling and inhibition in breast cancer. Curr Cancer Drug Targets 2009; 9:419-38.
2. Dean-Colomb W, Esteva FJ. Her2-positive breast cancer: Herceptin and beyond. Eur J Cancer 2008; 44:2806-12.
3. Sorlie T, Perou CM, Tibshirani R, Aas T, Geisler S, Johnsen H, et al. Gene expression patterns of breast carcinomas distinguish tumor subclasses with clinical implications. Proc Natl Acad Sci USA 2001; 98:10869-74.
4. Sorlie T, Tibshirani R, Parker J, Hastie T, Marron JS, Nobel A, et al. Repeated observation of breast tumor subtypes in independent gene expression data sets. Proc Natl Acad Sci USA 2003; 100:8418-23.
5. Murphy CG, Modi S. HER2 breast cancer therapies: A review. Biologics 2009; 3:289-301.
6. Hortobagyi GN. Trastuzumab in the treatment of breast cancer. N Engl J Med 2005; 353:1734-6.
7. Nahta R, Esteva FJ. HER2 therapy: Molecular mechanisms of trastuzumab resistance. Breast Cancer Res 2006; 8:215.
8. Lan KH, Lu CH, Yu D. Mechanisms of trastuzumab resistance and their clinical implications. Ann NY Acad Sci 2005; 1059:70-5.
9. Jin Q, Esteva FJ. Cross-talk between the ErbB/HER family and the type I insulin-like growth factor receptor signaling pathway in breast cancer. J Mammary Gland Biol Neoplasia 2008; 13:485-98.
10. Wang SE, Xiang B, Guix M, Olivares MG, Parker J, Chung CH, et al. Transforming growth factor beta engages TACE and ErbB3 to activate phosphatidylinositol-3 kinase/Akt in ErbB2-overexpressing breast cancer and desensitizes cells to trastuzumab. Mol Cell Biol 2008; 28:5605-20.
11. Neckers L. Heat shock protein 90 is a rational molecular target in breast cancer. Breast Dis 2002; 15:53-60.
12. Isaacs JS, Xu W, Neckers L. Heat shock protein 90 as a molecular target for cancer therapeutics. Cancer Cell 2003; 3:213-7.
13. Raja SM, Clubb RJ, Bhattacharyya M, Dimri M, Cheng H, Pan W, et al. A combination of trastuzumab and 17-AAG induces enhanced ubiquitinylation and lysosomal pathway-dependent ErbB2 degradation and cytotoxicity in ErbB2-overexpressing breast cancer cells. Cancer Biol Ther 2008; 7:1630-40.
14. Modi S, Stopeck A, Gordon MS, Solit D, Bagatell R, Flores S, et al. Trastuzumab and KOS-953 (17-AAG) is feasible and active in patients with metastatic breast cancer: Preliminary results of a phase 1/2 study. Presented at the 28th Annual San Antonio Breast Cancer Symposium December 8–11 2005, San Antonio TX.
15. Modi S, Stopeck AT, Gordon MS, Mendelson D, Solit DB, Bagatell R, et al. Combination of trastuzumab and tanespimycin (17-AAG, KOS-953) is safe and active in trastuzumab-refractory HER-2 overexpressing breast cancer: A phase I dose-escalation study. J Clin Oncol 2007; 25:5410-7.
16. Solit DB, Ivy SP, Kopil C, Sikorski R, Morris MJ, Slovin SF, et al. Phase I trial of 17-allylamino-17-demethoxygeldanamycin in patients with advanced cancer. Clin Cancer Res 2007; 13:1775-82.
17. Yano A, Tsutsumi S, Soga S, Lee MJ, Trepel J, Osada H, et al. Inhibition of Hsp90 activates osteoclast c-src signaling and promotes growth of prostate carcinoma cells in bone. Proc Natl Acad Sci USA 2008; 105:15541-6.
18. Hieronymus H, Lamb J, Ross KN, Peng XP, Clement C, Rodina A, et al. Gene expression signature-based chemical genomic prediction identifies a novel class of HSP90 pathway modulators. Cancer Cell 2006; 10:321-30.
19. Yang H, Chen D, Cui QC, Yuan X, Dou QP. Celastrol, a triterpene extracted from the chinese "thunder of god vine", is a potent proteasome inhibitor and suppresses human prostate cancer growth in nude mice. Cancer Res 2006; 66:4758-65.
20. Sethi G, Ahn KS, Pandey MK, Aggarwal BB. Celastrol, a novel triterpene, potentiates TNF-induced apoptosis and suppresses invasion of tumor cells by inhibiting NFkappaB-regulated gene products and TAK1-mediated NFkappaB activation. Blood 2007; 109:2727-35.
21. Abbas S, Bhoumik A, Dahl R, Vasile S, Krajewski S, Cosford ND, et al. Preclinical studies of celastrol and acetyl isogambogic acid in melanoma. Clin Cancer Res 2007; 13:6769-78.
22. Zhang T, Hamza A, Cao X, Wang B, Yu S, Zhan CG, et al. A novel Hsp90 inhibitor to disrupt Hsp90/Cdc37 complex against pancreatic cancer cells. Mol Cancer Ther 2008; 7:162-70.
23. Hassane DC, Guzman ML, Corbett C, Li X, Abboud R, Young F, et al. Discovery of agents that eradicate leukemia stem cells using an in silico screen of public gene expression data. Blood 2008; 111:5654-62.
24. Idris AI, Libouban H, Nyangoga H, Landao-Bassonga E, Chappard D, Ralston SH. Pharmacologic inhibitors of IkappaB kinase suppress growth and migration of mammary carcinosarcoma cells in vitro and prevent osteolytic bone metastasis in vivo. Mol Cancer Ther 2009; 8:2339-47.
25. Lee JH, Koo TH, Yoon H, Jung HS, Jin HZ, Lee K, et al. Inhibition of NFkappaB activation through targeting IkappaB kinase by celastrol, a quinone methide triterpenoid. Biochem Pharmacol 2006; 72:1311-21.
26. Trott A, West JD, Klaic L, Westerheide SD, Silverman RB, Morimoto RI, et al. Activation of heat shock and antioxidant responses by the natural product celastrol: Transcriptional signatures of a thiol-targeted molecule. Mol Biol Cell 2008; 19:1104-12.
27. Trachootham D, Alexandre J, Huang P. Targeting cancer cells by ROS-mediated mechanisms: A radical therapeutic approach? Nat Rev Drug Discov 2009; 8:579-91.
28. Malhotra JD, Kaufman RJ. Endoplasmic reticulum stress and oxidative stress: A vicious cycle or a double-edged sword? Antioxid Redox Signal 2007; 9:2277-93.
29. Tanner M, Kapanen AI, Junttila T, Raheem O, Grenman S, Elo J, et al. Characterization of a novel cell line established from a patient with herceptin-resistant breast cancer. Mol Cancer Ther 2004; 3:1585-92.
30. Roy V, Perez EA. Beyond trastuzumab: Small molecule tyrosine kinase inhibitors in HER-2-positive breast cancer. Oncologist 2009; 14:1061-9.
31. Yang H, Shi G, Dou QP. The tumor proteasome is a primary target for the natural anticancer compound withaferin A isolated from "indian winter cherry". Mol Pharmacol 2007; 71:426-37.
32. Sreeramulu S, Gande SL, Gobel M, Schwalbe H. Molecular mechanism of inhibition of the human protein complex Hsp90-Cdc37, a kinome chaperone-cochaperone, by triterpene celastrol. Angew Chem Int Ed Engl 2009; 48:5853-5.
33. Xu W, Marcu M, Yuan X, Mimnaugh E, Patterson C, Neckers L. Chaperone-dependent E3 ubiquitin ligase CHIP mediates a degradative pathway for c-ErbB2/Neu. Proc Natl Acad Sci USA 2002; 99:12847-52.
34. Zhou P, Fernandes N, Dodge IL, Reddi AL, Rao N, Safran H, et al. ErbB2 degradation mediated by the co-chaperone protein CHIP. J Biol Chem 2003; 278:13829-37.
35. Xu W, Yuan X, Jung YJ, Yang Y, Basso A, Rosen N, et al. The heat shock protein 90 inhibitor geldanamycin and the ErbB inhibitor ZD1839 promote rapid PP1 phosphatase-dependent inactivation of AKT in ErbB2 overexpressing breast cancer cells. Cancer Res 2003; 63:7777-84.

36. Srethapakdi M, Liu F, Tavorath R, Rosen N. Inhibition of Hsp90 function by ansamycins causes retinoblastoma gene product-dependent G_1 arrest. Cancer Res 2000; 60:3940-6.
37. Mimnaugh EG, Xu W, Vos M, Yuan X, Isaacs JS, Bisht KS, et al. Simultaneous inhibition of hsp 90 and the proteasome promotes protein ubiquitination, causes endoplasmic reticulum-derived cytosolic vacuolization and enhances antitumor activity. Mol Cancer Ther 2004; 3:551-66.
38. Fruehauf JP, Meyskens FL Jr. Reactive oxygen species: A breath of life or death? Clin Cancer Res 2007; 13:789-94.
39. Cheng G, Diebold BA, Hughes Y, Lambeth JD. Nox1-dependent reactive oxygen generation is regulated by Rac1. J Biol Chem 2006; 281:17718-26.
40. Zhang Q, Chatterjee S, Wei Z, Liu WD, Fisher AB. Rac and PI3 kinase mediate endothelial cell-reactive oxygen species generation during normoxic lung ischemia. Antioxid Redox Signal 2008; 10:679-89.
41. Westerheide SD, Bosman JD, Mbadugha BN, Kawahara TL, Matsumoto G, Kim S, et al. Celastrols as inducers of the heat shock response and cytoprotection. J Biol Chem 2004; 279:56053-60.
42. Roe SM, Prodromou C, O'Brien R, Ladbury JE, Piper PW, Pearl LH. Structural basis for inhibition of the Hsp90 molecular chaperone by the antitumor antibiotics radicicol and geldanamycin. J Med Chem 1999; 42:260-6.
43. Trachootham D, Zhou Y, Zhang H, Demizu Y, Chen Z, Pelicano H, et al. Selective killing of oncogenically transformed cells through a ROS-mediated mechanism by beta-phenylethyl isothiocyanate. Cancer Cell 2006; 10:241-52.
44. Radisky DC, Levy DD, Littlepage LE, Liu H, Nelson CM, Fata JE, et al. Rac1b and reactive oxygen species mediate MMP-3-induced EMT and genomic instability. Nature 2005; 436:123-7.
45. Nogueira V, Park Y, Chen CC, Xu PZ, Chen ML, Tonic I, et al. Akt determines replicative senescence and oxidative or oncogenic premature senescence and sensitizes cells to oxidative apoptosis. Cancer Cell 2008; 14:458-70.
46. Wang K, Fang H, Xiao D, Zhu X, He M, Pan X, et al. Converting redox signaling to apoptotic activities by stress-responsive regulators HSF1 and NRF2 in fenretinide treated cancer cells. PLoS One 2009; 4:7538.
47. Luo J, Solimini NL, Elledge SJ. Principles of cancer therapy: Oncogene and non-oncogene addiction. Cell 2009; 136:823-37.
48. Adams J. The proteasome as a novel target for the treatment of breast cancer. Breast Dis 2009; 15:61-70.
49. Tsukamoto S, Yokosawa H. Targeting the proteasome pathway. Expert Opin Ther Targets 2009; 13:605-21.
50. Neckers L. Heat shock protein 90 is a rational molecular target in breast cancer. Breast Dis 2009; 15:53-60.
51. Workman P, Burrows F, Neckers L, Rosen N. Drugging the cancer chaperone HSP90: Combinatorial therapeutic exploitation of oncogene addiction and tumor stress. Ann NY Acad Sci 2007; 1113:202-16.
52. Hwang M, Moretti L, Lu B. HSP90 inhibitors: Multitargeted antitumor effects and novel combinatorial therapeutic approaches in cancer therapy. Curr Med Chem 2009; 16:3081-92.
53. Singh S, Shi Q, Bailey ST, Palczewski MJ, Pardee AB, Iglehart JD, et al. Nuclear factorkappaB activation: A molecular therapeutic target for estrogen receptor-negative and epidermal growth factor receptor family receptor-positive human breast cancer. Mol Cancer Ther 2007; 6:1973-82.
54. Xia W, Bacus S, Husain I, Liu L, Zhao S, Liu Z, et al. Resistance to ErbB2 tyrosine kinase inhibitors in breast cancer is mediated by calcium-dependent activation of RelA. Mol Cancer Ther 2010; 9:292-9.
55. Band V, Zajchowski D, Swisshelm K, Trask D, Kulesa V, Cohen C, et al. Tumor progression in four mammary epithelial cell lines derived from the same patient. Cancer Res 1990; 50:7351-7.
56. Bonita DP, Miyake SLLM Jr, Langdon WY, Band H. Phosphotyrosine binding domain-dependent upregulation of the platelet-derived growth factor receptor alpha signaling cascade by transforming mutants of cbl: Implications for cbl's function and oncogenicity. Mol Cell Biol 1997; 17:4597-610.
57. Solit DB, Zheng FF, Drobnjak M, Munster PN, Higgins B, Verbel D, et al. 17-allylamino-17-demethoxygeldanamycin induces the degradation of androgen receptor and HER-2/neu and inhibits the growth of prostate cancer xenografts. Clin Cancer Res 2002; 8:986-93.